CERN-TH/2002-263
SLAC-PUB-9580

NNLL QCD Corrections to the Decay $B \to X_s \ell^+ \ell^-$

A. Ghinculov [a], T. Hurth [b,c,1], G. Isidori [d], Y.-P. Yao[e]

[a] *Department of Physics and Astronomy*
UCLA, Los Angeles CA 90095-1547, USA

[b] *Theoretical Physics Division, CERN, CH-1211 Genève 23, Switzerland*

[c] *SLAC, Stanford University, Stanford, CA 94309, USA*

[d] *INFN, Laboratori Nazionali di Frascati, I-00044 Frascati, Italy*

[e] *Randall Laboratory of Physics*
University of Michigan, Ann Arbor MI 48109-1120, USA

Abstract

We briefly discuss the status of the NNLL QCD calculations in the inclusive rare B decay $B \to X_s \ell^+ \ell^-$. Two important ingredients, the two-loop matrix elements of the four quark operator $\mathcal{O}_2$ and the bremsstrahlung contributions, were quite recently finalised. The new contributions significantly improve the sensitivity of the inclusive decay $B \to X_s l^+ l^-$ decay in testing extensions of the standard model in the sector of flavour dynamics; for instance the two-loop calculation cuts the low-scale uncertainty in half and the bremsstrahlung calculation leads to a 10% shift of the position of the zero of the forward-backward asymmetry.

[1] Heisenberg Fellow

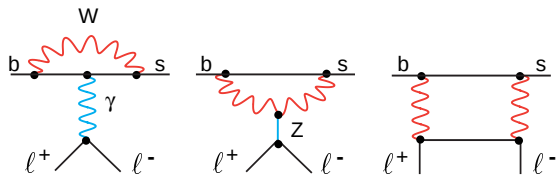

Figure 1: The decay $B \to X_s l^+ l^-$ at one-loop.

1 The Decay $B \to X_s \ell^+ \ell^-$

Inclusive rare B decays like $B \to X_s \gamma$ or $B \to X_s \ell^+ \ell^-$ are very important tools to understand the nature of physics beyond the Standard Model (SM). The stringent bounds obtained from $B \to X_s \gamma$ on various non-standard scenarios (see e.g. [1, 2, 3]) are a clear example of the importance of theoretically clean FCNC observables in discriminating new-physics models.

In comparison with the $B \to X_s \gamma$, the inclusive $B \to X_s \ell^+ \ell^-$ decay presents a complementary and also more complex test of the SM

since different contributions add to the decay rate, see fig. 1. Quite recently, BELLE announced the first measurement of the inclusive mode [4].

Generally, inclusive rare decay modes of the B meson are theoretically clean observables. For instance the decay width $\Gamma(B \to X_s \gamma)$ is well approximated by the partonic decay rate $\Gamma(b \to s\gamma)$, which can be analysed in renormalization-group-improved perturbation theory. Non-perturbative contributions play only a subdominant role and can be calculated in a model-independent way by using the heavy-quark expansion. However, in the decay $B \to X_s \ell^+ \ell^-$ there are also on-shell $c\bar{c}$ resonances. While in the decay $B \to X_s \gamma$ (on-shell photon) the intermediate ψ background for example, namely $B \to \psi X_s$ followed by $\psi \to X' \gamma$, is suppressed and can be subtracted from the $B \to X_s \gamma$ decay rate, the $c\bar{c}$ resonances in the decay $B \to X_s l^+ l^-$ (off-shell photon) show up as large peaks in the dilepton invariant mass spectrum. These resonances can be removed by appropriate kinematic cuts in the invariant mass spectrum. In the 'perturbative windows', namely in the low-dilepton mass region $s = (p_{\ell^+} + p_{\ell^-})^2/mb^2 < 0.25$ and also in the high-dilepton mass region with $0.65 < s$, theoretical predictions for the invariant mass spectrum are dominated by the purely perturbative contributions, and theoretical precision comparable with the one reached in the decay $B \to X_s \gamma$ is possible. In the decay $B \to X_s \ell^+ \ell^-$ kinematic observables such as the invariant dilepton mass spectrum and the forward-backward (FB) asymmetry are particularly attractive, especially for the search for physics beyond the SM. These observables are usually normalized by the semileptonic decay rate in order to reduce the uncertainties due to bottom quark mass and CKM angles. The normalized dilepton invariant mass spectrum and the FB asymmetry are defined as

$$R(s) = \frac{d}{ds}\Gamma(B \to X_s \ell^+ \ell^-)/\Gamma(B \to X_c e \bar{\nu}), \tag{1.1}$$

$$A_{\rm FB}(s) = \Gamma(B \to X_c e \bar{\nu}) \times \\ \times \int_{-1}^{1} d\cos\theta_\ell \, \frac{d^2\Gamma(B \to X_s \ell^+ \ell^-)}{ds \; d\cos\theta_\ell} \mathrm{sgn}(\cos\theta_\ell), \tag{1.2}$$

where θ_ℓ is the angle between ℓ^+ and B momenta in the dilepton centre-of-mass frame.

The B factories will soon provide statistics and resolution needed for the measurements of $B \to X_s \ell^+ \ell^-$ kinematic distributions. Precise theoretical estimates of the SM expectations are therefore needed in order to perform new significant tests of flavour physics.

2 NNLL QCD Corrections

Within inclusive B decay modes, short-distance QCD corrections lead to a sizeable modification of the pure electroweak contribution, generating large logarithms of the form $\alpha_s^n(m_b)$ $\log^m(m_b/M_{\rm heavy})$, where $m \leq n$ (with $n = 0, 1, 2, ...$). A suitable framework to achieve the necessary resummations of these large logs is the construction of an effective low-energy theory with five quarks, obtained by integrating out the heavy degrees of freedom,

$$H_{eff} = -\frac{4G_F}{\sqrt{2}}\,\lambda_t \sum_{i=1}^{10} C_i(\mu)\,\mathcal{O}_i(\mu) \quad . \tag{2.3}$$

Compared with the decay $B \to X_s\gamma$, the effective Hamiltonian (2.3) contains the two additional operators of order $O(\alpha_{\rm em})$, $\mathcal{O}_9$ and $\mathcal{O}_{10}$:

$$\begin{array}{ll} \mathcal{O}_1 = & (\bar{s}\gamma_\mu T^a P_L c)\,(\bar{c}\gamma^\mu T_a P_L b) \\ \mathcal{O}_2 = & (\bar{s}\gamma_\mu P_L c)\,(\bar{c}\gamma^\mu P_L b) \\ \mathcal{O}_7 = & e/16\pi^2\, m_b(\mu)\,(\bar{s}\sigma^{\mu\nu} P_R b)\,F_{\mu\nu} \\ \mathcal{O}_8 = & g_s/16\pi^2\, m_b(\mu)\,(\bar{s}\sigma^{\mu\nu} T^a P_R b)\,G^a_{\mu\nu} \\ \mathcal{O}_9 = & e^2/16\pi^2\,(\bar{s}\gamma_\mu P_L b)\,(\bar{\ell}\gamma^\mu \ell) \\ \mathcal{O}_{10} = & e^2/16\pi^2\,(\bar{s}\gamma_\mu P_L b)\,(\bar{\ell}\gamma^\mu \gamma_5 \ell) \end{array} \tag{2.4}$$

The four-quark operators $\mathcal{O}_{3..6}$ are not given explicitly because of their numerically small Wilson coefficients.

Within this framework, QCD corrections are twofold: corrections related to the Wilson coefficients, and those related to the matrix elements of the various operators, both evaluated at the low-energy scale $\mu \approx m_b$. As the heavy fields are integrated out, the top-quark-, W-, and Z-mass dependence is contained in the initial conditions of the Wilson coefficients, determined by a matching procedure between full and effective theory at the high scale. By means of RG equations, the $C_i(\mu, M_{\rm heavy})$ are then evolved at the low scale. Finally, the QCD corrections to the matrix elements of the operators are evaluated at the low scale.

Because the first large logarithm of the form $\log(m_b/m_W)$ arises already without gluons due to the mixing of the four-quark operator $\mathcal{O}_2$ into $\mathcal{O}_9$ at one loop, the leading logarithms sum (LL) and the next-to-leading logarithms sum (NLL) are given by

$$\begin{array}{ll} \text{LL} & [\alpha_{\rm em}\,\log(m_b/M)]\;\alpha_s^n(m_b)\;\log^n(m_b/M) \\ \text{NLL} & [\alpha_{\rm em}\,\log(m_b/M)]\;\alpha_s^{n+1}(m_b)\;\log^n(m_b/M)\,. \end{array}$$

The complete NLL contributions to the decay amplitude can be found in [7, 8]. Since the LL contribution to the rate turns out to be numerically rather small, NLL terms represent an $O(1)$ correction to this observable. On the other hand, since a non-vanishing FB asymmetry is generated by the interference of vector ($\sim \mathcal{O}_{7,9}$) and axial-vector ($\sim \mathcal{O}_{10}$) leptonic currents, the LL amplitude leads to a vanishing result and NLL terms represent the lowest non-trivial contribution to this observable.

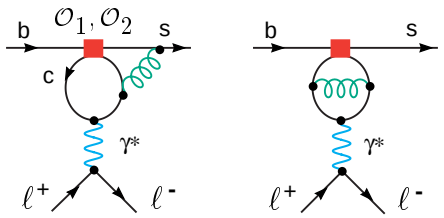

Figure 2: Typical diagrams (finite parts) contributing to the matrix element of the operator $\mathcal{O}_{1,2}$ at the NNLL level

For these reasons, a computation of NNLL terms in $B \to X_s\ell^+\ell^-$ is needed if one aims at the same numerical accuracy as achieved by the NLL analysis of $B \to X_s\gamma$. Large parts of the latter can be taken over and used in the NNLL calculation of $B \to X_s\ell^+\ell^-$. However, this is not the full story.

The full computation of initial conditions o the renormalization group equation to NNLL precision has been presented in Ref. [10] some time ago - including a confirmation of the $b \to s\gamma$ NLL matching results of [11]. The inclusion of this NNLL contribution removes the large matching scale uncertainty (around 16%) of the NLL calculation of the $b \to s\ell^+\ell^-$ decay rate.

Most of the NNLL contributions to the anomalous-dimension matrix can be derived from the NLL analysis of $b \to s\gamma$ [9]. The missing entries are estimated to have a small numerical influence on the dilepton mass spectrum [10] and do not contribute to the FB asymmetry.

There are two further important ingredients of the NNLL program which were recently calculated, namely the two-loop matrix elements of the four-quark operators $\mathcal{O}_{1,2}$ and the NNLL bremsstrahlung contributions which will be discussed in the following sections.

In principle, a complete NNLL calculation of the $B \to X_s\ell^+\ell^-$ rate would require also the calculation of two-loop matrix element of the operator $\mathcal{O}_9$. However, its impact to the dilepton mass spectrum is also estimated to be very small. Similarly to the missing piece of the anomalous-dimension matrix, also this (scale-independent) contribution does not enter the FB asymmetry at NNLL accuracy.

3 Two-loop Matrix Elements of $\mathcal{O}_{1,2}$

Within the $B \to X_s\gamma$ calculation at NLL, the two-loop matrix elements of the four-quark operator $\mathcal{O}_2$ for an on-shell photon were calculated in [12] using Mellin-Barnes techniques. This calculation was extended in [5] to the case of an off-shell photon (see fig. 2) with the help of a double Mellin-Barnes representation which corresponds to a NNLL contribution relevant to the decay $B \to X_s\ell^+\ell^-$. This leads to a double expansion in the dilepton mass s and the mass ratio m_c^2/m_b^2. Thus, the validity of these analytical results given in [5] is restricted to small dilepton masses $s < 0.25$.

An independent check of these results has been performed by us [15]. Moreover, our NNLL calculation [15] is also valid for high dilepton masses for which the experimental methods have much higher efficiency compared to the one at low dilepton masses [4].

In our approach [15], the following calculational method was used: First all diagrams were

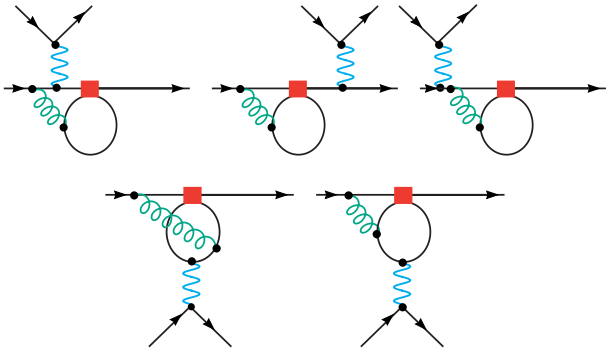

Figure 3: Two gauge-invariant subset, without (up) and with (down) a nontrivial $c\bar{c}$ threshold.

converted into sums of sun-set type integrals and their mass derivatives,

$$\int d^n p\, d^n q\, \frac{p^{\mu_1} \dots p^{\mu_i} q^{\mu_{i+1}} \dots q^{\mu_j}}{((p+k)^2 + m_1^2)(q^2 + m_2^2)(r^2 + m_3^2)}$$

where $r = p + q$. The effective masses $m^2_{1,2,3}$ and the effective momentum k are polynomial functions of physical masses, external kinematics, and Feynman parameters associated with the diagrams. Integrations over the Feynman parameters are understood. After the internal momenta p and q are integrated over, one can show that the results can be spanned by a finite set of ten scalar kernels, which are functions of $m^2_{1,2,3}$ and k^2 in one-dimensional integral representations, multiplied by tensors made of the metric and k. The Feynman parameters are extended into the complex plane to effect rapid numerical convergence. In principle, possible IR singularities have to be isolated and substracted. However, an important simplification within this specific calculation is given by the fact that all relevant two-loop diagrams are IR finite.

It is clear that a nontrivial $c\bar{c}$ threshold behaviour at the NNLL level cannot be reproduced by the expansion method used in [5]. This easily explains our results of the comparison of the two independent calculations, [5] and [15], within the low-s-region. The Mellin-Barnes expansion of the gauge-invariant subset shown in fig. 3 are in excellent agreement with our numerical results. We found that the expanded results given in [5] are even valid beyond the claimed validity range $s < 0.25$. In contrast, this is not true for the second gauge-invariant subset given in fig. 3 because of the nontrivial $c\bar{c}$ threshold in that case. In [5] it was already shown that in the low-dilepton mass region these NNLL contributions reduce the perturbative uncertainty (due the low-scale dependence) from $\pm 13\%$ down to $\pm 6.5\%$ and also the central value is changed significantly, $\sim 14\%$.

There is no additional problem due to the charm mass renormalisation scheme ambiguity within the decay $B \to X_s \ell^+ \ell^-$ because the charm dependence starts already at one-loop in contrast to the case of the decay $B \to X_s \gamma$. The charm dependence itself leads to a $\sim 7\%$ uncertainty. These small uncertainties in the inclusive mode should be compared with the ones of the correspondung exclusive mode $B \to K^* \mu^+ \mu^-$ given in [13]; $\Delta BR = (^{+26}_{-17}, \pm 6, ^{+6}_{-4}, ^{-0.7}_{+0.4}, \pm 2)\%$. The first dominating error represents the hadronic uncertainty due to the formfactors.

A phenomenolgical NNLL analysis including the high dilepton mass region will be presented in [15].

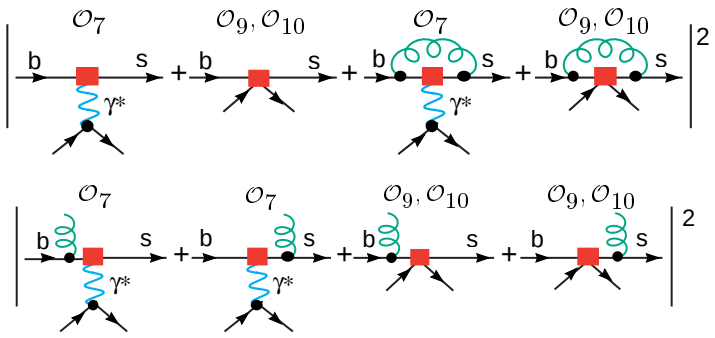

Figure 4: Virtual (up) and real (down) QCD corrections.

4 Bremsstrahlung Contributions

The NNLL bremsstrahlung contributions were also recently calculated for the dilepton mass spectrum (symmetric part) in [6, 14] and for the FB asymmetry in [14, 16], see fig. 4.

In [14] we have separated the bremsstrahlung corrections into universal and nonuniversal pieces. We defined the terms $\sigma_{7,9}(s)$ which take into account *universal* $O(\alpha_s)$ bremsstrahlung corrections as $O(\alpha_s)$ corrections of the effective Wilson coefficients by demanding that the remaining (finite) non-universal bremsstrahlung corrections of the rate (encoded in the functions τ_{77} and τ_{99}) vanish in the limit $s \to 1$. Then the universal contributions take into account the truly soft component of the radiation, which diverges at the $s \to 1$ boundary of the phase space. This is because in the $s \to 1$ limit only the soft component of the radiation survives and, according to Low's theorem, the latter gives rise to a correction proportional to the tree-level matrix element. In [14] we then found that *all* nonuniversal bremsstrahlung corrections τ_i, to the rate and to the FB asymmetry, are rather small all over the phase space, and particularly for large values of s ($|\tau_i(s)| < 0.5$ for $s > 0.3$), in comparison with the dominating universal corrections.

In the case of the forward–backward asymmetry there are ambiguities arising for $d \neq 4$ in the definition of γ_5 but in the case of the decay rate, the problematic γ_5 contribution vanishes because of the $p_1 \leftrightarrow p_2$ permutation symmetry of the leptonic phase space. To circumvent this problem, we employed the following hybrid regularization scheme [14]: the Dirac algebra of IR-divergent pieces is strictly treated in four dimensions (dimensional reduction), while the virtual UV-divergent pieces, which do not involve any γ_5 ambiguity, are still computed in naïve dimensional regularization. For example, the hybrid wave function renormalization constant for a massless quark is given by $Z_\psi^{m=0} = 1 - \frac{\alpha_s}{4\pi}\frac{4}{3}\left(\frac{1}{\epsilon_{\rm UV}} - \frac{1}{\epsilon_{\rm IR}} - 1\right)$. At this level of the perturbative expansion, this hybrid regularization scheme is gauge invariant. Using this scheme we were able to explicitly verify the cancellation of IR divergences in our bremsstrahlung calculation [14]. However, anticipating the cancellation of IR-divergences, one also can circumvent the γ_5 ambiguity by calculating only finite bremsstrahlung contributions [16].

Let us finally discuss the phenomenological impact of these bremsstarhlung calculations - focusing on the position of the zero of the FB asymmetry. This quantity, defined by $A_{\rm FB}(s_0) = 0$, is particularly interesting to determine relative sign and magnitude of the Wilson coefficients C_7 and C_9 and it is therefore extremely sensitive to possible new physics effects.

The NLL result $s_0^{\rm NLL} = 0.14 \pm 0.02$ where the error is determined by the scale dependence

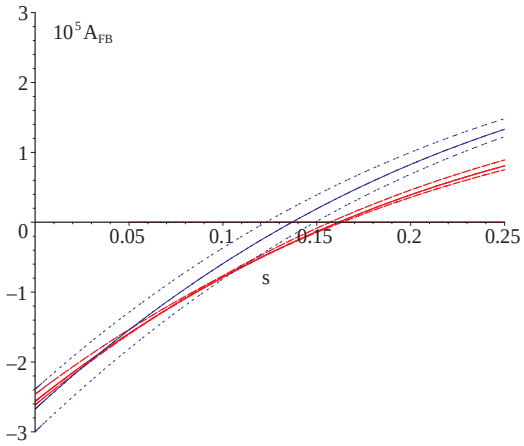

Figure 5: Comparison between NNLL and NLL results for $A_{\rm FB}(s)$ in the low s region. The three thick (red) lines are the NNLL predictions for $\mu = 5$ GeV (full), and $\mu = 2.5$ and 10 GeV (dashed); the dotted (blue) curves are the corresponding NLL results. All curves for $m_c/m_b = 0.29$.

(2.5 GeV $\leq \mu \leq$ 10 GeV) is now modified by the discussed NNLL contributions to (see fig. 5)

$$s_0^{\rm NNLL} = 0.162 \pm 0.008 \ . \tag{4.5}$$

In this case the variation of the result induced by the scale dependence is accidentally very small (about $\pm 1\%$ for 2.5 GeV $\leq \mu \leq$ 10 GeV) and cannot be regarded as a good estimate of missing higher-order effects. Taking into account the separate scale variation of both Wilson coefficients $C_9^{\rm new}$ and $C_7^{\rm new}$, and the charm-mass dependence, we estimate a conservative overall error on s_0 of about 5% [14]. In this s-region the nonperturbative $1/m_b^2$ and $1/m_c^2$ corrections to $A_{\rm FB}(s)$ are very small and also under control. Summing up, the zero of the FB asymmetry in the inclusive mode turns out to be one of the most sensitive tests for new physics beyond the SM.

References

[1] G. D'Ambrosio, G.F. Giudice, G. Isidori and A. Strumia, arXiv:hep-ph/0207036; G. Degrassi, P. Gambino and G. F. Giudice, *JHEP* **0012** (2000) 009; M. Carena, D. Garcia, U. Nierste and C. E. Wagner, *Phys. Lett.* **B 499** (2001) 141.

[2] F. Borzumati, C. Greub, T. Hurth and D. Wyler, *Phys. Rev.* **D 62** (2000) 075005; T. Besmer, C. Greub and T. Hurth, *Nucl. Phys.* **B 609** (2001) 359.

[3] T. Hurth, in *Proc. 5th Int. Symposium on Radiative Corrections (RADCOR 2000)* ed. H.E. Haber, arXiv:hep-ph/0106050.

[4] BELLE Collab., arXiv:hep-ex/0208029.

[5] H. H. Asatrian, H. M. Asatrian, C. Greub and M. Walker, *Phys. Rev.* **D 65** (2002) 074004.

[6] H. H. Asatryan, H. M. Asatrian, C. Greub and M. Walker, arXiv:hep-ph/0204341.

[7] M. Misiak, *Nucl. Phys.* **B 393** (1993) 23.

[8] A. J. Buras and M. Munz, *Phys. Rev.* **D 52** (1995) 186.

[9] K. Chetyrkin, M. Misiak and M. Munz, *Phys. Lett.* **B 400** (1997) 206.

[10] C. Bobeth, M. Misiak and J. Urban, *Nucl. Phys.* **B 574** (2000) 291.

[11] K. Adel and Y. Yao, *Phys. Rev.* **D 49** (1994) 4945; C. Greub and T. Hurth, *Phys. Rev.* **D 56** (1997) 2934.

[12] C. Greub, T. Hurth and D. Wyler, *Phys. Lett.* **B 380** (1996) 385; *Phys. Rev.* **D 54** (1996) 3350.

[13] A. Ali, P. Ball, L. T. Handoko and G. Hiller, Phys. Rev. D **61**, 074024 (2000).

[14] A. Ghinculov, T. Hurth, G. Isidori and Y.-P. Yao, arXiv:hep-ph/0208088.

[15] A. Ghinculov, T. Hurth, G. Isidori and Y.-P. Yao, in preparation.

[16] H. M. Asatrian, K. Bieri, C. Greub and A. Hovhannisyan, arXiv:hep-ph/0209006.